THE JOURNAL OF BIOLOGICAL CHEMISTRY
Vol. 276, No. 15, Issue of April 13, pp. 11902–11912, 2001

Printed in U.S.A.

Probing the Determinants of Coenzyme Specificity in Ferredoxin-NADP$^+$ Reductase by Site-directed Mutagenesis*

Received for publication, October 11, 2000, and in revised form, November 21, 2000
Published, JBC Papers in Press, January 4, 2001, DOI 10.1074/jbc.M009287200

Milagros Medina‡§, Alejandra Luquita‡¶, Jesús Tejero‡, Juan Hermoso‖, Tomás Mayoral‖, Julia Sanz-Aparicio‖, Koert Grever‡, and Carlos Gómez-Moreno‡

From the ‡Departamento de Bioquímica y Biología Molecular y Celular, Facultad de Ciencias, Universidad de Zaragoza, 50009 Zaragoza and ‖Grupo de Cristalografía Macromolecular y Biología Estructural, Instituto Química-Física Rocasolano, Consejo Superior de Investigaciones Científicas, Serrano 119, 28006 Madrid, Spain

On the basis of sequence and three-dimensional structure comparison between *Anabaena* PCC7119 ferredoxin-NADP$^+$ reductase (FNR) and other reductases from its structurally related family that bind either NADP$^+$/H or NAD$^+$/H, a set of amino acid residues that might determine the FNR coenzyme specificity can be assigned. These residues include Thr-155, Ser-223, Arg-224, Arg-233 and Tyr-235. Systematic replacement of these amino acids was done to identify which of them are the main determinants of coenzyme specificity. Our data indicate that all of the residues interacting with the 2′-phosphate of NADP$^+$/H in *Anabaena* FNR are not involved to the same extent in determining coenzyme specificity and affinity. Thus, it is found that Ser-223 and Tyr-235 are important for determining NADP$^+$/H specificity and orientation with respect to the protein, whereas Arg-224 and Arg-233 provide only secondary interactions in *Anabaena* FNR. The analysis of the T155G FNR form also indicates that the determinants of coenzyme specificity are not only situated in the 2′-phosphate NADP$^+$/H interacting region but that other regions of the protein must be involved. These regions, although not interacting directly with the coenzyme, must produce specific structural arrangements of the backbone chain that determine coenzyme specificity. The loop formed by residues 261–268 in *Anabaena* FNR must be one of these regions.

During the last decades, the understanding of protein function and, more specifically, the role of the individual amino acid residues involved in substrate binding and in the catalytic action have achieved considerable progress. Among the most relevant enzymes studied are those involved in electron transfer processes due to their practical importance. Now, the opportunity to design novel proteins is becoming more feasible, especially due to the increased detailed knowledge of the three-dimensional structure of many proteins. As a first step in this direction recent investigations have been aimed to redesign already existing proteins, so that they can produce a function different to that for which they were naturally synthesized (1, 2). Following this direction, a lot of effort is being made in the description of the determinants of coenzyme specificity for NAD(P)$^+$/H-dependent redox enzymes (3–5). In biological systems NAD$^+$/H is almost exclusively used by enzymes that catalyze oxidative exergonic reactions, whereas reductive endergonic reactions are generally catalyzed by enzymes that utilize NADP$^+$/H (6). However, the only structural difference between them is the presence of a 2′-P group bound to the AMP moiety of the coenzyme in NADP$^+$/H, and it is the presence or the absence of this phosphate group that permits the enzymes to make the distinction between these two coenzymes. Moreover, among the structurally related enzymes of the FNR family, members with preference either for NADP$^+$/H or NAD$^+$/H can be found. Crystallographic studies have demonstrated that discrimination between these coenzymes does not result from the presence of different structural domains in these enzymes (7–9).

We describe the introduction of point mutations in the coenzyme binding domain of ferredoxin-NADP$^+$ reductase (FNR,[1] EC 1.18.1.2) from the cyanobacterium *Anabaena* PCC7119 to probe the determinants of its coenzyme specificity and also as an initial attempt to alter the coenzyme specificity. This enzyme consists of a soluble single polypeptide chain that contains a noncovalently bound FAD group that is the cofactor involved in the redox reaction. Several points prompted us to choose FNR. During photosynthesis FNR accepts electrons from ferredoxin and uses them to convert NADP$^+$ into NADPH (10). This process is highly specific for NADP$^+$/H *versus* NAD$^+$/H (11–13). Extensive biochemical characterization of FNR from different sources and, in particular, from *Anabaena* has been carried out (11–23), and several three-dimensional structures of FNR forms are available (24–26). Moreover, the structural arrangement of FNR has been proposed to be the prototype of a family of flavin oxidoreductases that interact specifically with either NADP$^+$/H or NAD$^+$/H (8, 25, 27). Finally, considering the high economical value of the reduced form of NADP$^+$/H, the development of an *in vitro* system using FNR to generate NADPH is of high interest. Work is already

* This work was supported by Comisión Interministerial de Ciencia y Tecnología, Spain Grant BIO97-0912C02-01 (to C. G.-M.). The costs of publication of this article were defrayed in part by the payment of page charges. This article must therefore be hereby marked "*advertisement*" in accordance with 18 U.S.C. Section 1734 solely to indicate this fact.

The atomic coordinates and structure factors (code 1bqe) have been deposited in the Protein Data Bank, Research Collaboratory for Structural Bioinformatics, Rutgers University, New Brunswick, NJ (http://www.rcsb.org/).

§ Recipient of a travel award to the University of Cambridge from the Caja de Ahorros de la Inmaculada-Consejo Superior de Investigación y Desarrollo. To whom correspondence should be addressed: Departamento de Bioquímica y Biología Molecular y Celular. Facultad de Ciencias. Universidad de Zaragoza, Pedro Cerbuna 12, 50009 Zaragoza, Spain. Tel.: 34 976 762476; Fax: 34 976 762123; E-mail: mmedina@posta.unizar.es.

¶ Recipient of a travel award to the Universidad de Zaragoza from Universidad Nacional de Rosario and a grant from the Spanish Government. Present address: Cátedra de Física Biológica, Departamento de Ciencias Fisiológicas, Facultad de Ciencias Médicas, Santa Fé 3100, 2000 Rosario, Argentina.

[1] The abbreviations used are: FNR, ferredoxin-NADP$^+$ reductase; DCPIP, 2,6-dichlorophenolindophenol; 2′-P, 2′-phosphate; WT, wild type.

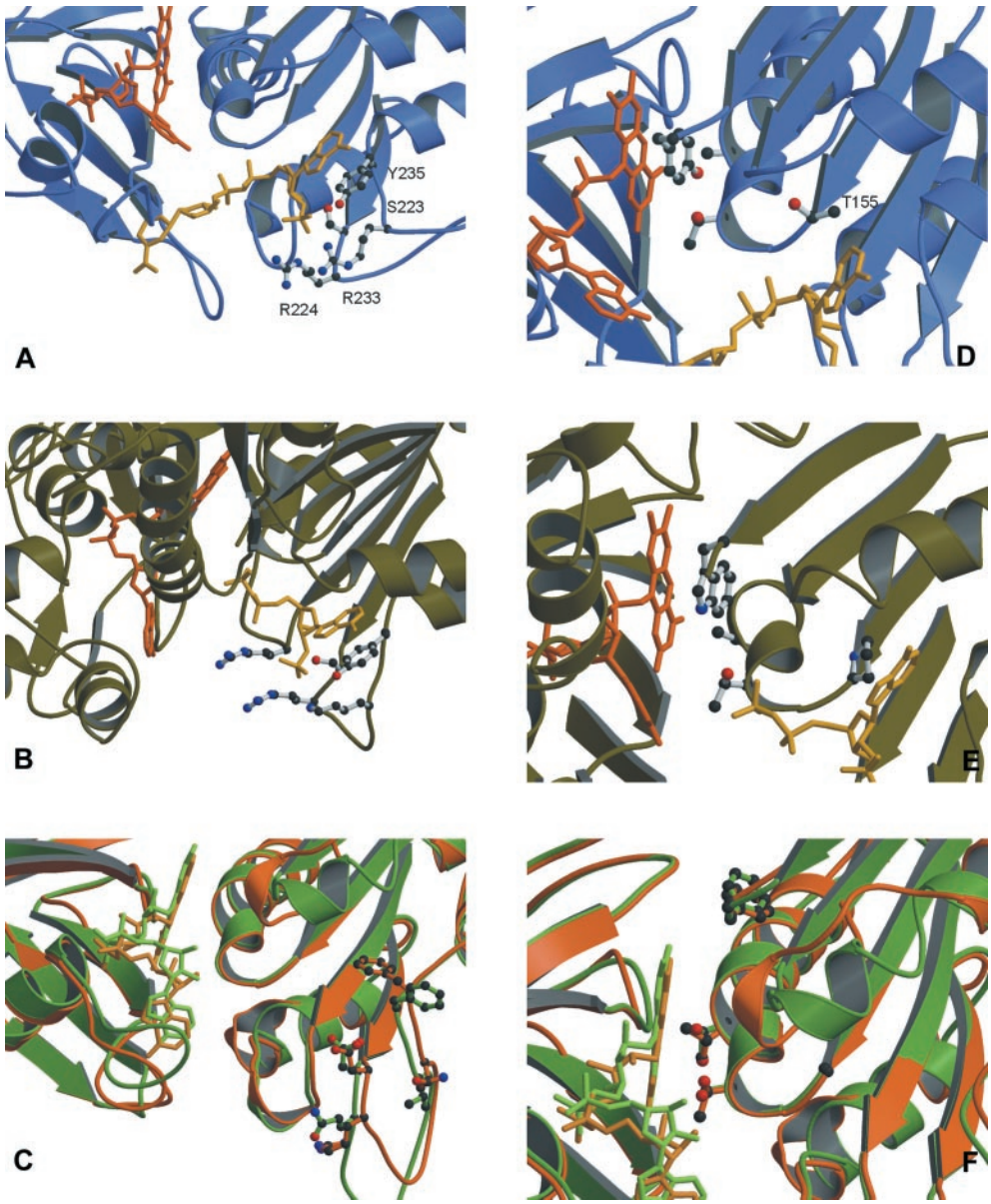

FIG. 1. **Three-dimensional structure comparison of the FNR family in the regions involved in the coenzyme binding.** *Anabaena* FNR is shown in *A* and *D*, and NADPH cytochrome P450 reductase is shown in *B* and *E*. NAD^+/H-dependent reductases are shown in *C* and *F*, and they are represented by corn nitrate reductase (*orange*) and NADH-cytochrome b_5 reductase (*green*). The region interacting with the 2′-phosphate of $NADP^+$ is compared in *A*, *B*, and *C*. In the FNR and other $NADP^+$/H-dependent enzymes, this region has two (FNR) or three (NADPH cytochrome-P450 reductase) positively charged residues, respectively, stabilizing the negative charge of the phosphate group; this group is also hydrogen-bonded to Ser-223 and a Tyr-235 residues (*A* and *B*). In the case of NAD^+/H enzymes (*C*) these residues are not conserved. The region interacting with the pyrophosphate of the coenzyme presents a different consensus sequence depending on the coenzyme, NADPH (*D* and *E*) or NADH (*F*). In $NADP^+$/H-dependent enzymes Thr-155 (Pro), Thr-157, and Ala-160 (*Anabaena* FNR numbering) are always conserved (*D* and *E*). In those interacting with NAD^+/H, the equivalent residues are Gly, *X*, and Thr (*F*). The FAD cofactor and the coenzyme (if present) are drawn as *sticks*. Flavin cofactor are colored *orange*, and $NADP^+$/H analogues are colored *yellow*. This figure was drawn using MOLSCRIPT (61) and RENDER (62).

under progress in this direction, and we foresee this development occurring in the near future (28). If we also achieve change of coenzyme specificity for FNR, generation of NADH could also be obtained with the same system. Moreover, due to the much cheaper value of NADH *versus* NADPH, the system could be used in the opposite direction, with NADH as reducing power, to produce reduced proteins (like ferredoxin, flavodoxin, hydrogenase, cytochrome P450 reductase, etc.).

Different crystallographic approaches on a variety of FNR forms from different sources have provided a picture of how the $NADP^+$ substrate must bind to FNR (24–26). Thus, the studies of spinach and *Anabaena* FNR revealed the importance of the side chains of residues Arg-100, Ser-223, Arg-224, Arg-233, Tyr-235, and Gln-237 (*Anabaena* FNR numeration) in the stabilization of the complex with $NADP^+$/H by making contacts to its adenine ring, its 2′-P, and its 5′-phosphoryl (24, 25). The negative charge of the 2′-P group is apparently stabilized by the lateral chains of two positive-charged arginine residues, Arg-224 and Arg-233 (Arg-235 and Lys-244 in the spinach enzyme). The 2′-P of $NADP^+$/H might also form hydrogen bonds with Ser-223 and Tyr-235 (in this case a stacking interaction is also formed with the adenine moiety of $NADP^+$/H) (Fig. 1*A*). The sequence and three-dimensional structure of FNR at the site of $NADP^+$ interaction have been compared with those of several $NADP^+$ and NAD^+ reductases within the FNR family (Table I, Fig. 1). Conservation of residues interacting with the 2′-P group of $NADP^+$/H was observed. Thus, Ser-223, Arg-224, Arg-233, and Tyr-235 are conserved or show

TABLE I

Sequence alignment of different members of the FNR family in three of the conserved sequence regions involved in coenzyme binding

Residue numbers are shown at the left and right of each sequence. Hyphens denote gaps introduced to improve alignment. FNR, *Anabaena* PCC7119, ferredoxin-NADP$^+$ reductase from *Anabaena* PCC7119 (50); FNR, pea, ferredoxin-NADP$^+$ reductase from pea (51); FNR, spinach, ferredoxin-NADP$^+$ reductase from spinach (52); CYP450R, rat cytochrome-P450 reductase (53); SiR, sulfite reductase from *E. coli* (54); NOS, human neuronal nitric-oxide synthase (55); NR, corn root, maize root nitrate reductase (56); NR, corn leaf, maize leaf nitrate reductase (57); Cb5R, bovin, bovin cytochrome b_5 reductase (58); Cb5R, pig, pig cytochrome b_5 reductase (59); PDR, phthalate dioxygenase reductase from *Pseudomonas cepacia* (60). Positions mutated in the present study, and those equivalent in the other sequences, are shown in bold.

NADPH-dependent enzymes												
FNR, *Anabaena* PCC7119	150	VIML**A**T**G**TGI**A**PM	162	220	YAI**SR**---EQKNPQGG**R**M**Y**IQ	237	257	HTYICGLR-GMEE-GIDAAL	274
FNR, pea	159	VIMLG**T**GTGI**A**PF	171	225	FAV**SR**---EQVNDKGE**K**M**Y**IQ	242	262	FVYMCGLK-GMEK-GIDDIM	279
FNR, spinach	165	IIMLG**T**GTGI**A**PF	177	229	FAV**SR**---EQTNEKGE**K**M**Y**IQ	246	268	YFYMCGLK-GMEK-GIDDIM	285
CYP450R, rat	527	VIMVG**P**GTGI**A**PF	539	592	VAF**SR**---EQAH----**K**V**Y**VQ	605	625	HIYVCGDARNMAKDVQNT-F	643
SiR, *E. coli*	454	VIMIG**P**GTGI**A**PF	466	515	LAW**SR**---DQKE----**K**V**Y**VQ	528	647	HIYVCGDANRMAKDVEQA-L	565
NOS, human	1249	CILVG**P**GTGI**A**PF	12611315		TAY**SR**---EPDKP---**K**K**Y**VQ	13291350		HIYVCGDV-TMAADVLKAIQ	1368
NADPH, NADH-dependent enzymes												
NR, corn root	102	LAMIQ**A**GRGT**T**PD	114	165	YVV**SK**VP--EDGWEYG**V**G**R**VD	183	199	IALVCGPP-AMIECTVRPGL	217
NADH-dependent enzymes												
NR, corn leaf	490	LAMIC**G**GSGI**T**PM	502	553	YVI**DQ**VKRPEEGWKYS**V**G**F**VT	573	589	LALACGPP-PMIQFAISPNL	607
Cb5R, bovin	174	VGMIA**G**GTGI**T**PM	186	236	YTV**DK**---APEAWDYS**Q**G**F**VN	253	269	LVLMCGPP-PMIQYACLPNL	287
Cb5R, pig	146	VGMIA**G**GTGI**T**PM	158	208	YTV**DR**---APEAWDYS**Q**G**F**VN	225	241	LVLMCGPP-PMIQYACLPNL	259
PDR, *P. cepacia*	114	FILVA**G**GIGI**T**PM	126	170	IHH**DH**---GDP----------	177	195	HVYCCGPQALMDT-VRDMTG	213

conservative substitutions in all the NADP$^+$/H-depending enzymes (Fig. 1*B*, Table I). However, in the NAD$^+$/H-dependent enzymes, these residues are not conserved, which interrupts the stabilization of 2′-P group and probably modifies the stacking interaction with the adenine moiety of NADP$^+$/H by changing Tyr-235 by Phe (Fig. 1*C*). Sequence and structure analysis suggest that other regions of the protein might also account for FNR coenzyme specificity (Table I, Fig. 1, *D–F*). Thus, most of the members of the FNR family that bind NADP$^+$/H show the sequence T(P)GTGXAP (residues 155–161 in *Anabaena* FNR; whereas in those interacting with NAD$^+$/H, the corresponding sequence is GGXGXTP (Table I). These residues form the loop between β1 and α-helix A as well as the first residues of this α-helix, whose N-terminal end might stabilize an interaction with the negative pyrophosphate of the coenzyme (Fig. 1*D*). A similar motif has also been shown to exist in the case of the flavoenzyme glutathione reductase, which is not a member of the FNR family and to be involved in coenzyme specificity (3). To confirm the importance of the interactions with the 2′-P group of NADP$^+$ and of the TGTGXAP FNR motive in *Anabaena* FNR coenzyme specificity, the T155G, S223G, S223D, R224Q, R233A, Y235F, and Y235A *Anabaena* FNR mutants have been constructed and characterized by a variety of techniques. The choice of the introduced mutations has been made taking into account the residues that occupy the equivalent positions in the NAD$^+$/H-dependent members of the FNR family and trying to simulate a potential change in cofactor specificity (Table I). The rest of the mutations have been analyzed as controls. Moreover, after a careful analysis of the three-dimensional structure recently reported for a complex between FNR and ferredoxin (29), none of these residues is expected to be involved in ferredoxin binding or electron transfer.

EXPERIMENTAL PROCEDURES

Oligonucleotide-directed Mutagenesis—Anabaena FNR mutants were prepared using a construct of the *pet*H gene previously cloned into the expression vector pTrc99a as a template (30). The FNR mutants T155G, S223D, S223G, R224Q, R233A, Y235F, and Y235A were produced using the Transformer site-directed mutagenesis kit from CLONTECH in combination with suitable synthetic oligonucleotides. The pTrc99a vectors with the desired mutation were used to transform the *Escherichia coli* Pasteur collection strain 0225 (17).

Purification of the FNR Mutants—FNR mutants were purified from isopropyl-1-thio-β-D-galactopyranoside-induced LB cultures as described previously (17, 30). Some of the mutants were not retained by the Cibacron blue gel and were purified by fast protein liquid chromatography using a Mono-Q column. UV-visible spectra and SDS-polyacrylamide gel electrophoresis were used as purity criteria.

Spectral Analysis—Ultraviolet-visible spectral analyses were carried out either on a Hewlett-Packard diode array 8452 spectrophotometer, a Kontron Uvikon 860 spectrophotometer, or a Kontron Uvikon 942 spectrophotometer. Circular dichroism was carried out on a Jasco 710 spectropolarimeter at room temperature in a 1-cm path length cuvette. Protein concentrations were 0.7 μM for the far UV and 3 μM for the aromatic and visible regions of the spectrum. Photoreduction of different FNR forms was performed at room temperature in an anaerobic cuvette containing 32–65 μM FNR samples and 3 μM 5-deazariboflavin in 50 mM Tris/HCl buffer, pH 8. The solutions were made anaerobic by repeated evacuation and flushing with O_2-free Ar. The spectra were recorded in a HP8452 diode array spectrophotometer before and after irradiating the samples with a 300-W light source for different times. Dissociation constants of the complexes between oxidized FNR mutants and either NADP$^+$ or NAD$^+$ were measured by differential spectroscopy using a double beam spectrophotometer at 25 °C as previously described (12, 17).

Enzymatic Assays—Diaphorase activity, assayed with DCPIP as artificial electron acceptor was determined for all the FNR mutants as described previously (17). Both NADPH and NADH were assayed as coenzyme electron donors to each of the different FNR mutants. Unless otherwise stated, all the measurements were carried out in 50 mM Tris/HCl, pH 8.0. In all measurements, direct reduction of DCPIP by the coenzyme was subtracted from that of the enzyme-coenzyme mixture. The kinetic results obtained from the diaphorase activity were interpreted using the Michaelis-Menten kinetic model. In the case of the diaphorase reactions studied using NADH, high enzyme concentrations (0.5–9 μM) were required to detect and follow their activity. Therefore, in some of these cases the coenzyme concentration used was only 100 times higher than that of the corresponding enzyme. This was also the case for the S223D FNR form with NADPH, where the enzyme concentration in the cuvette was 1 μM. When assaying the reaction of the other FNR enzymes with NADPH, enzyme concentrations ranging from 3 to 25 nM were used.

Stopped-flow Kinetic Measurements—Fast electron transfer processes between NADPH or NADH and the different FNR_{ox} mutants were studied by stopped-flow methodology under anaerobic conditions using an Applied Photophysics SX17.MV spectrophotometer interfaced with an Acorn 5000 computer using the SX.17MV software of Applied Photophysics as previously described (17). The observed rate constants (k_{obs}) were calculated by fitting the data to a mono- or bi-exponential equation. Samples were made anaerobic (in specially designed tonometers that fit the stopped-flow apparatus) by successive evacuation and flushing with O_2-free Ar in 50 mM Tris/HCl, pH 8.0. Final FNR concentrations were kept between 6 and 11 μM, whereas, unless otherwise stated, NADPH final concentrations were in the range of 160–200 μM, and NADH was used at final concentrations in the range of 250–300 μM or at 2.5 mM. The same methodology was also applied to the study of the reduction of NADP$^+$ by T155G FNR_{rd}. The time course of the reactions was followed at 460 nm, although other wavelengths were also analyzed (340 and 600 nm).

Crystal Growth, Data Collection, and Structure Refinement—Crystals of the T155G FNR mutant were grown by the hanging drop method. The 5-μl droplets consisted of 2 μl of 25.9 mg of protein/ml of solution

TABLE II
Data collection and refinement statistics
r.m.s., root mean square.

Data collection	
Temperature (K)	291
Source	Rotating anode
Space group	P65
Cell *a*, *b*, *c* (Å)	88.13, 88.13, 97.25
Resolution range (Å)	40.1–2.4
No. of unique reflections	15,728
Completeness of data (%)	
All data	99.5
Outer shell	97.2
R_{sym} [a]	0.10
Refinement statistics	
Sigma cutoff	
Resolution range (Å)	9.0–2.4
No. of protein atoms	2335
No. of heterogen atoms	58
No. of solvent atoms	267
R-factor[b]	0.16
Free *R*-factor	0.24
r.m.s. deviation	
Bond lengths (Å)	0.014
Bond angles (degree)	1.4

[a] $R_{sym} = \Sigma hkl\ \Sigma_i|I_i - \langle I\rangle|/\Sigma hkl\ \Sigma_i\langle I\rangle$.
[b] $R\text{-factor} = \|F_o| - |F_c\|/|F_o|$.

buffered with 10 mM Tris/HCl, pH 8.0, 1 μl of unbuffered β-octylglucoside at 5% (w/v), and 2 μl of reservoir solution containing 18% (w/v) polyethylene glycol 6000, 20 mM ammonium sulfate, and 0.1 M sodium acetate, pH 5.0. The droplet was equilibrated against 1 ml of reservoir solution at 20 °C. Under these conditions crystals grew within 1–7 days up to a maximum size of (0.8 × 0.4 × 0.4 mm) in the presence of a phase separation caused by the detergent.

These crystals were mounted in glass capillaries and screened on a Mar Research (Germany) image plate area detector for intensity, resolution, and mosaic spread using graphite-monochromated CuKα radiation generated by an Enraf-Nonius rotating anode generator. X-ray data for the T155G FNR were collected at 20 °C to a maximum resolution of 2.4 Å. Crystals belong to the $P6_5$ hexagonal space group with the following unit cell dimensions: $a = b = 88.13$ Å and c = 97.25 Å. The V_M is 3.0 Å^3/Da with one FNR molecule in the asymmetric unit and 60% solvent content. The x-ray data set was processed with MOSFLM (31) and scaled and reduced with SCALA from the CCP4 package (32).

The T155G structure was solved by molecular replacement using the program AmoRe (33) on the basis of the 1.8-Å resolution native FNR model (24) without the FAD cofactor. An unambiguous single solution for the rotation and translation functions was obtained. This solution was refined by the fast rigid-body refinement program FITING (34). The model was subjected to alternate cycles of conjugate gradient refinement with the program X-PLOR (35) and manual model building with the software package O (36). The crystallographic *R* and R_{free} (37) values converged to values of 0.16 and 0.24, respectively for reflections between 9.0- and 2.4-Å resolution (Table II). The final model contains 2335 nonhydrogen protein atoms and 1 FAD, 1 SO_4^{2-}, and 267 solvent molecules. The atomic coordinates of the T155G FNR mutant have been deposited in the Protein Data Bank (code 1bqe).

RESULTS

Expression and Purification of the Different FNR Mutants—The level of expression in *E. coli* of all the mutated FNR forms was judged to be similar to that of the recombinant WT. All the mutants were obtained in homogeneous form and in amounts suitable to perform the demanding characterization studies described herein. Mutants at the position of Ser-223 interacted weakly with the Cibacron blue column, which binds specifically those proteins with a $NAD(P)^+$/H interaction site, requiring the use of a fast protein liquid chromatography Mono-Q column for purification.

Spectral Properties—No major differences were detected in the UV-visible absorption and CD spectra of any of the FNR forms (Fig. 2). Therefore, no major structural perturbations appear to have been introduced by the mutations, and the extinction coefficient of *Anabaena* WT FNR (9.4 $mM^{-1}\ cm^{-1}$ at 458 nm) (38) has been assumed herein for all the FNR mutants. Illumination of the FNR forms in the presence of 5-deazariboflavin caused the reduction of the protein to the neutral FNR semiquinone form with maxima in the range of 520 and 588–595 nm for all the FNR mutants (Fig. 2*B*). As for the WT enzyme, isosbestic points are also detected around 364 and 507 nm for the oxidized-semiquinone transition for all the mutants. Under the assayed conditions WT FNR stabilizes only 22% semiquinone. However, although a similar amount of semiquinone form is stabilized by most of the mutants, S223G and S223D showed an unexpected increment in the proportion of the radical stabilization (34 and 43%, respectively).

Steady-state Kinetics of the Different FNR Forms—The steady-state kinetic parameters of the different FNR mutants were analyzed for the DCPIP-diaphorase reaction using either NADPH or NADH as electron donor (Table III). T155G, R224Q, and Y235F yielded similar values for k_{cat} in the NADPH-dependent reaction to the WT enzyme. This parameter decreased by a factor of 4, 2, and 4 for S223G, R233A, and Y235A, respectively, and was up to 200 times smaller in the case of the S223D FNR form. With regard to the K_m value for NADPH, T155G, R224Q, and Y235F showed moderated increments with regard to the WT enzyme value (about 4-, 13-, and 7-fold), whereas S223G, R233A, and Y235A yielded much higher K_m values for NADPH (about 50-, 36-, and 67-fold, respectively), with S233D being the mutant with the highest K_m value (about 125-fold larger) (Table III). Taking into account the kinetic parameters obtained, all the mutants showed a significantly decreased catalytic efficiency (k_{cat}/K_m) with regard to the WT FNR. The introduction of an aspartic acid residue at position 223 was the mutation that most affected the catalytic efficiency of the enzyme with NADPH (Fig. 3*A*).

The DCPIP-diaphorase activity of the WT and all the FNR mutants was also assayed with NADH as electron donor (Table III). The data indicate that, in terms of both k_{cat} and K_m, NADH is a very poor reductant for WT FNR (k_{cat} decreased 38-fold, and K_m for the coenzyme increased by a factor of 133 with respect to NADPH). Therefore, *Anabaena* FNR has a very low catalytic efficiency with NADH (Table III), and the specificity of the enzyme for NADPH, expressed as the ratio between the catalytic efficiency for NADPH and NADH, was found to be 67,000 times higher (Fig. 3). Although all the mutants presented a k_{cat} value for the NADH-dependent reaction within a factor of 10 with regard to that of WT FNR, R224Q, R233A, and Y235F show a clear increase of this value (4–7-fold), whereas T155G and Y235A show a decrease (about 7–8-fold) (Table III). It is noteworthy that these two mutants, T155G and Y235A, are the only ones showing a decrease in the K_m value for NADH (about 4- and 2-fold respectively), whereas the rest of the mutants show an increment for this parameter to within a factor of 4 of the WT value. As is also shown in Table III, the catalytic efficiency of all these mutants with NADH is within a factor of 10 that of the WT enzyme with this coenzyme and for all of them is considerably smaller than that observed with NADPH (Fig. 3). However, it is noteworthy that when Ser-223 is replaced by an aspartic acid, the catalytic efficiency with NADPH approximates that obtained with NADH. Thus, the S223D single mutation decreases the enzyme specificity for NADPH from 67,000 times in the WT to only 8 times in the mutant (Fig. 3*A*).

Interaction of FNR Mutants with $NADP^+$ and NAD^+— The interaction of the different FNR forms with either $NADP^+$ or NAD^+ was investigated by differential spectroscopy (Fig. 4). When $NADP^+$ binds to oxidized WT FNR, the visible spectrum

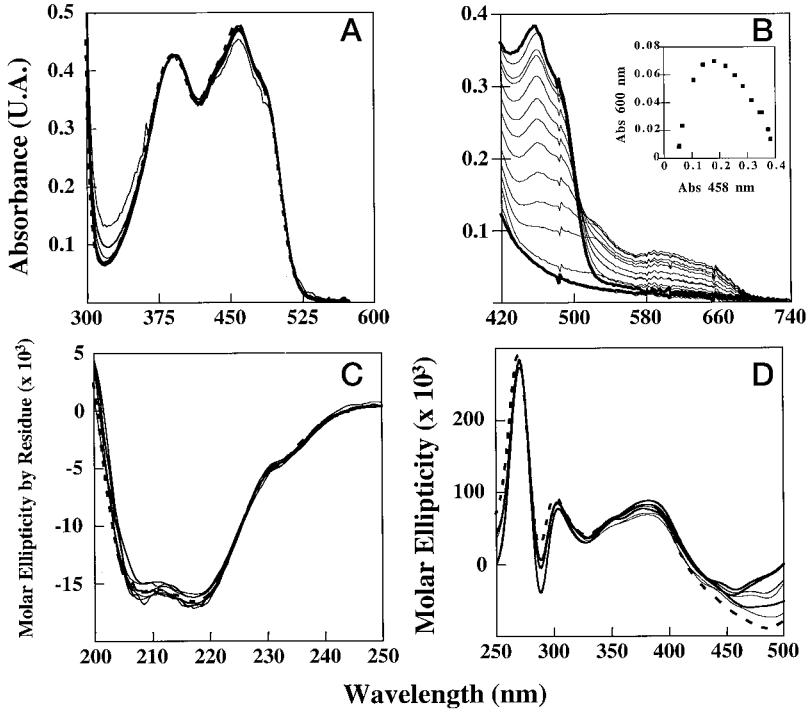

FIG. 2. **Spectral properties.** (*A*) Superposition of the absorption spectra of WT FNR (*dotted bold*) and the different mutated FNR forms in the visible region. (*B*) Photoreduction of S223D FNR in the presence of 3 μM dRf. The inset shows the production of the semiquinone form absorbance (600 nm) *vs* that of the oxidized and reduced protein (458 nm). Absorption spectra were recorded in 50 mM Tris/HCl, pH 8.0 at room temperature. Circular dichroism spectra of WT (*dotted bold*) and mutated FNR forms in the (*C*) far-ultraviolet and the (*D*) near-ultraviolet and visible regions of the spectrum. All the CD spectra were recorded in 1 mM Tris/HCl, pH 8.0 at room temperature.

TABLE III
Steady-state kinetic parameters for the diaphorase activity with DCPIP of wild-type and mutated FNR forms from Anabaena

FNR form	K_m NADPH	k_{cat} NADPH	k_{cat}/K_m NADPH	K_m NADH	k_{cat} NADH	k_{cat}/K_m NADH
	μM	s^{-1}	$s^{-1} \cdot \mu M^{-1}$	μM	s^{-1}	$s^{-1} \cdot \mu M^{-1}$
WT	6.0 ± 0.6[a]	81.5 ± 3.0[a]	13.5[a]	800 ± 50	0.16 ± 0.02	2×10^{-4}
T155G	23 ± 3	97.3 ± 0.5	4.23	178 ± 14	0.019 ± 0.002	1.6×10^{-4}
S223G	300 ± 35	20 ± 1	0.067	1300 ± 100	0.18 ± 0.02	1.4×10^{-4}
S223D	760 ± 100	0.38 ± 0.03	5×10^{-4}	3500	0.22 ± 0.02	6×10^{-5}
R224Q	83 ± 11	83 ± 1	1	2600	1.1 ± 0.1	4×10^{-4}
R233A	216 ± 30	42 ± 30	0.19	2500	0.70 ± 0.02	2.8×10^{-4}
Y235F	41 ± 3	93 ± 3	2.2	1400 ± 200	0.63 ± 0.02	4.5×10^{-4}
Y235A	400 ± 40	17.5 ± 0.6	0.044	475 ± 60	0.023 ± 0.002	5×10^{-5}

[a] Data from Medina *et al.* (17).

of the bound flavin undergoes a perturbation, yielding the difference spectrum shown in Fig. 4*A*. This has been shown in the case of the *Anabaena* FNR to be due to the interaction of the 2′,5′-ADP moiety of the cofactor with the reductase (12). The spectral perturbations observed for oxidized R224Q, R233A, and Y235F FNRs upon $NADP^+$ binding were weaker but very similar in shape to those observed for the WT FNR, and only minor displacements of the minima (around 392 and 502 nm) and maxima (around 354, 458, 480, and 522 nm) were detected (Fig. 4, *A* and *B*). The difference spectra obtained at different coenzyme concentrations allowed the determination of the dissociation constants and binding energies for the corresponding complexes (Fig. 4*F*, Table IV) (12). Thus, Y235F, R224Q, and R233A bind $NADP^+$ 35-, 95-, and 210-fold weaker than the WT FNR. Therefore, although binding of $NADP^+$ to either Y235F, R224Q, or R233A FNRs produce equivalent structural perturbations around the flavin ring as those observed for the WT, apparently the positive side chains of Arg-224 and Arg-233 play an active role in positioning the coenzyme by making direct contacts with it. Interestingly, binding of $NADP^+$ to T155G FNR elicited spectral changes at different wavelengths than those reported for WT FNR (Fig. 4*D*), with minima at 396 and 440 nm and maxima around 476 and 512 nm, whereas the binding was estimated to be only 17-fold weaker than that of the WT (Table IV). This result indicates that, although Thr-155 might not be directly involved in the interaction with the coenzyme, the replacement of Thr-155 by Gly produced slight structural changes in the protein that have an important influence in the arrangement of the flavin environment when the coenzyme is bound. Finally, when oxidized S223D, S223G, and Y235A FNR forms were titrated with $NADP^+$, no difference spectra were detected in the flavin region of the spectra as shown in Fig. 4*E* for Y235A. These mutants were only characterized by a loss of absorbance peaking in the 334–338 nm range, which allowed estimation of very high values for the dissociation constants in the case of these complexes (Table IV), indicating the importance of positions Ser-223 and Tyr-235 in coenzyme recognition and binding.

It has already been shown that NAD^+ is not able to produce any spectral perturbation in the flavin absorption range when added to WT FNR, presumably due to the absence of the 2′-P group, which is essential for $NADP^+$ binding to *Anabaena* FNR (12). When the mutants were titrated with NAD^+, only T155G elicited a weak difference spectrum in the flavin region with maxima at 420 and 505 nm (Fig. 4*C*). These data indicate that replacement of Thr-155 by Gly produced some changes in the protein that allow NAD^+ to perturb the FAD environment of FNR. No difference spectra were obtained with any other FNR mutant in the flavin region of the spectra.

Fast Kinetic Studies of the Reduction of FNR Mutants by NADPH and NADH—The fast kinetic reaction of oxidized *Anabaena* FNR forms with either NADPH or NADH was de-

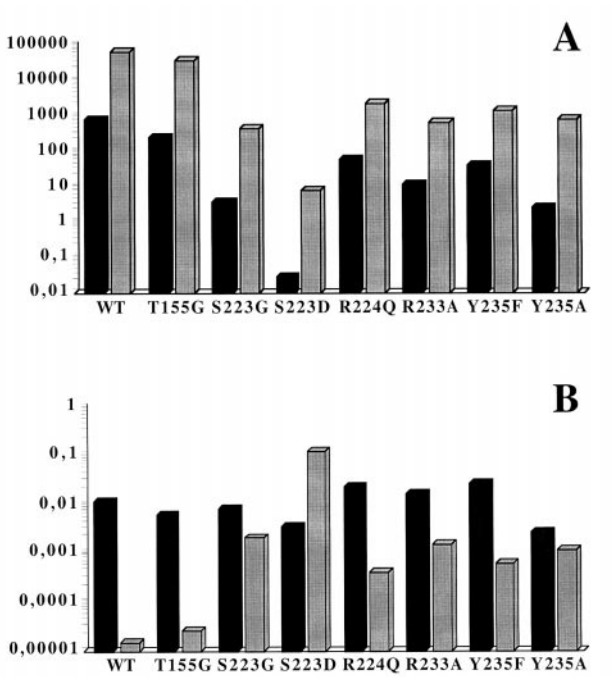

FIG. 3. **Comparison of the DCPIP-diaphorase activity kinetic parameters of WT and mutated FNR forms.** *A*, catalytic efficiency ($\mu M^{-1}\ s^{-1}$, *black columns*) and specificity for NADPH (*gray columns*). *B*, catalytic efficiency ($\mu M^{-1}\ s^{-1}$, *black columns*) and specificity for NADH (*gray columns*). Specificity for a coenzyme is defined as the ratio between its catalytic efficiency and that for the other coenzyme.

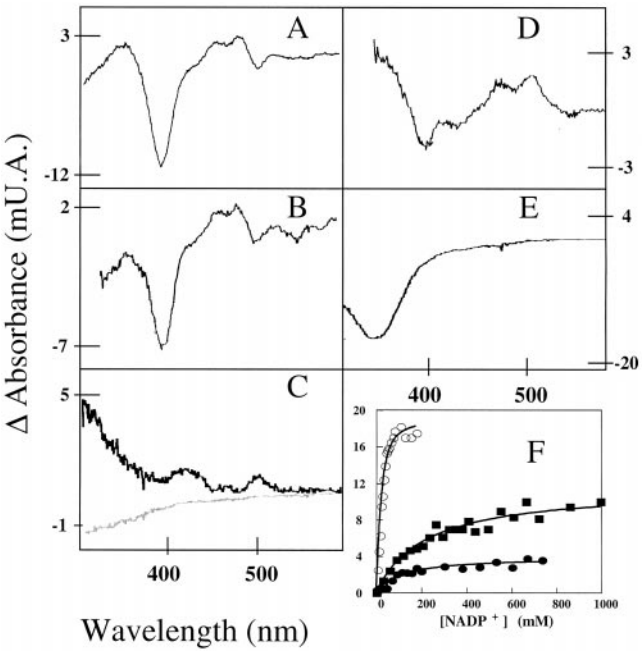

FIG. 4. **Spectroscopic characterization of the complexes between the FNR_{ox} forms and the coenzymes $NADP^+$ or NAD^+.** Difference absorbance spectra elicited by binding of (*A*) WT FNR (25 μM) to $NADP^+$ (60 μM), (*B*) Y235F FNR (20 μM) to $NADP^+$ (500 μM), (*C*) T155G FNR (19 μM) to NAD^+ (4.5 mM) and in grey WT FNR (20 μM) to NAD^+ (4.5 mM) (D) T155G FNR (24 μM) to $NADP^+$ (740 μM) and (*E*) Y235A FNR (23 μM) to $NADP^+$ (2 mM). The spectra were recorded at 25 °C in 50 mM Tris/HCl, pH 8.0. (*F*) Spectrophotometric titration of selected FNR forms with $NADP^+$. *Open circles*, WT FNR; *filled squares*, Y235F FNR; *filled circles*, T155G FNR.

termined by following the flavin spectral changes at 340, 460, and 600 nm under anaerobic conditions. As already reported (17), WT *Anabaena* FNR reacted rapidly with NADPH, producing a decrease in the absorption at 460 nm that was best fit by two processes that have been attributed to the production of the charge-transfer complex [FNR_{ox}-NADPH] ($k_{obs} > 500\ s^{-1}$) followed by the hydride transfer from NADPH to FAD ($k_{obs} \sim 200\ s^{-1}$), resulting in the equilibrium mixture of both charge-transfer complexes, [FNR_{ox}-NADPH] and [FNR_{rd}-$NADP^+$] (39). The time course for the kinetics of the reaction of T155G, R224Q, and Y235F FNR forms with NADPH were similar to that of the WT enzyme observed at 460 nm (Fig. 5*A*), and fitting of the experimental kinetic traces showed only slightly slower k_{obs} values for charge-transfer complex formation and hydride transfer with NADPH than those observed for the WT enzyme reaction (Table V). However, when analyzing the reaction of NADPH with S223G, S223D, R233A, or Y235A FNR forms, much longer time scales were required to complete the reaction and to reach an equivalent decay amplitude of the FNR absorbance at 460 nm (Fig. 5*B*). Moreover, the observed kinetics for these mutants were best fit to mono-exponential processes having k_{obs} values that were lower than those of the WT enzyme by 30-fold for Y235A and S223G, 330-fold for R233A, and 1500-fold for S223D (Table V). Taking into account the K_d values reported in Table IV, complex formation must be the rate-limiting process for these FNR forms, since this reaction is much slower than the subsequent electron transfer reaction whose rate constant, therefore, cannot be estimated. Measurements were also carried out at 340 and 600 nm to get a better knowledge of the observed processes (not shown). It is noteworthy that, although only negligible absorbance changes were observed at these wavelengths for the kinetics of the reaction of WT, T155G, R224Q, and Y235F FNR forms with NADPH corresponding to the kinetics observed at 460 nm, much slower processes can be detected at 340 and 600 nm, with similar amplitudes and time scales for all the FNR forms assayed. For the moment we do not have an explanation for these observations, but additional work is being done in the general characterization of the catalytic mechanism of this system that exceeds the scope of the present study.

In the case of the T155G FNR form, the kinetics of reoxidation of the enzyme by $NADP^+$ has also been studied by stopped-flow. An increase in absorbance at 460 nm due to FNR reoxidation and an increase at 340 nm due to NADPH formation were observed (Fig. 6). The traces were well fit by a single exponential having a rate constant of at least $350\ s^{-1}$. This behavior is similar to that reported for the WT enzyme for which a k_{obs} greater than $550\ s^{-1}$ has been reported when analyzed under similar conditions (17).

When analyzing the reaction of WT FNR with NADH by stopped-flow a very slow decrease in the absorption at 460 nm was observed that was best fit by two processes having k_{obs}

TABLE IV
Dissociation constants and free energy for complex formation of different Anabaena PCC 7119 FNR forms in the oxidized state with $NADP^+$ and NAD^+

FNR form	K_d^{NADP+}	$\Delta G^{o\ NADP+}$	K_d^{NAD+}	$\Delta G^{o\ NAD+}$
	μM^{-1}	$kcal \cdot mol^{-1}$	μM^{-1}	$kcal \cdot mol^{-1}$
WT	5.7 ± 0.3^a	-7.10 ± 0.05^a	ND[b]	
T155G	99 ± 10	-5.50 ± 0.06	ND[c]	
S223G	>8000		ND[b]	
S223D	ND[b]		ND[b]	
R224Q	535 ± 20	-4.44 ± 0.02	ND[b]	
R233A	1200	−4.2	ND[b]	
Y235F	200 ± 20	-5.00 ± 0.04	ND[b]	
Y235A	ND[b]		ND[b]	

[a] Data from Medina *et al.* (17).
[b] No difference spectra were detected in the flavin wavelength range.
[c] Spectral perturbations were too weak even at high coenzyme concentration.

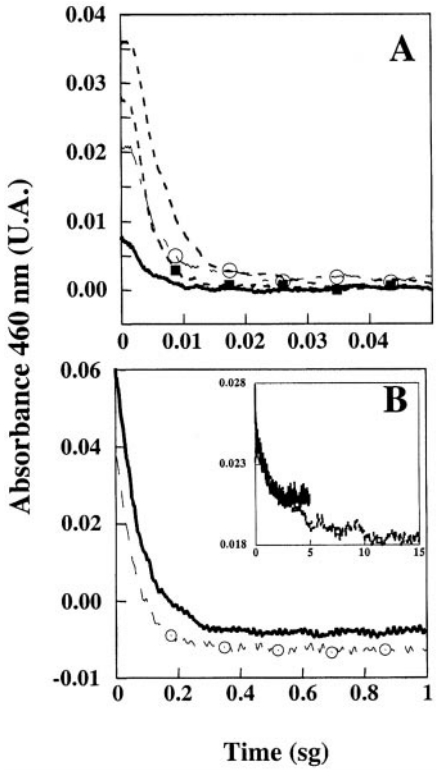

FIG. 5. **Time course of the anaerobic reactions of the different FNR forms with NADPH observed at 460 nm.** *A*, 6 μM WT FNR_{ox} (*bold line*) reacted with 170 μM NADPH, 9 μM T155G FNR_{ox} (*closed squares*) reacted with 160 μM NADPH, 9 μM R224Q FNR_{ox} (*dotted line*) reacted with 190 μM NADPH, 6 μM Y235F FNR_{ox} (*open circles*) reacted with 170 μM NADPH. *B*, 9 μM S223G FNR_{ox} (*open circles*) reacted with 240 μM NADPH, 11 μM S223D FNR_{ox} (*open squares*) reacted with 160 μM NADPH, 6.5 μM R233A FNR_{ox} (*closed squares*) reacted with 2.5 mM NADPH, 15 μM Y235A FNR_{ox} (*bold line*) reacted with 240 μM NADPH. Reactions were carried out in 50 mM Tris/HCl, pH 8.0, at 13 °C. Final concentrations are given. *U.A.*, units of absorbance.

values of 0.35 (~60% amplitude) and 0.005 (~40% amplitude) s^{-1} (Fig. 7*A*, Table V). Reaction of NADH with R224Q, R233A, and Y235F took place with k_{obs} values that were within a factor of 2–5 that obtained for the WT enzyme (Table V, Fig. 7*B*). However, although R224Q and R233A were best fit to a monoexponential process, two processes were observed for the Y235F mutant, which shows an important increase in the second k_{obs} value while maintaining the same amplitude relationships observed for the WT reaction. On the contrary, reaction of NADH with T155G, S223D, or Y235A FNR forms required longer time scales to reach equivalent decay amplitudes of the FNR absorbance at 460 nm (Fig. 7, *B* and *C*, Table V), and therefore, these mutants yield observed rate constants smaller than those detected for the WT enzyme. Interestingly, the decay observed for the reaction of NADH with T155G FNR shows the beginning of the second process delayed with regard to the first one (Fig. 7*C*). It is noteworthy that we have already observed this behavior for some reactions of the different FNR forms when working at lower coenzyme concentrations and that for some of the other mutants (Y235F, S223D for example) a very small lag phase can be also observed at high NADH concentration (Fig. 7). These processes were also analyzed at 600 nm (Fig. 7), where all the mutants showed an increase in absorbance followed by a decay to above the initial base line. The first processes observed are consistent in most of the cases with the one observed at 460 nm. However, T155G FNR shows a different behavior, with the final decay observed for the other FNR forms at 600 nm replaced by a second, delayed absorbance increase that is consistent with that observed at 460 nm (Fig. 7*C*, *inset*). Thus far, as was the case for the reactions with NADPH at long time scales, we do not have a good explanation for all the observed processes. Surely the observed changes in absorbance would reflect the association and interconversion of the $NAD(P)^+$/H-FNR forms, and further work along these lines is under way and will be reported elsewhere. However, comparison of the data obtained for the different FNR forms, including the WT enzyme, provides valuable information in the present study.

Three-dimensional Structure of the T155G FNR Mutant—After observing the difference spectra for the T155G FNR mutant in the presence of $NADP^+$, which indicated a slightly different structural arrangement of the flavin environment in the presence of the coenzyme, we decided to determine the three-dimensional structure of the T155G FNR form by x-ray diffraction. The first eight residues in the sequence were not included in the model due to the poor electron density map in this region. The overall folding of the T155G FNR mutant shows no significant differences with respect to the native structure, as shown by the low root-mean-square deviations (0.4 Å) of the Cα backbone of the mutant superimposed on the native FNR backbone (Fig. 8). Prominent differences are concentrated in the loop starting at Tyr-104 and ending at Val-113 near the region interacting with the adenine moiety of FAD, but they are not significant due to the poor definition of the electron density map in this region for all FNR forms. No structural changes in the Cα backbone at the mutated position were observed. This is surely a consequence of the fact that strand 1, in which residue 155 is located, is strongly stabilized by strands 2 and 4 of the β-sheet. Furthermore, the turn connecting the end of this first strand with the succeeding α-helix is stabilized by one hydrogen bond between Thr-157 and the OH group of the Tyr-303 (see Fig. 1*D*). However, structural differences are observed in the Thr-155 environment (positions 261–268) (Fig. 8). This region corresponds to the turn linking strand 4 to the beginning of α-helix D of the $NADP^+$ binding domain. The structural changes in the mutated enzyme can be explained on the basis of the altered hydrogen bond network of this region after mutation (Table VI and Fig. 9). The Thr-155 to Gly-155 mutation essentially eliminates two interactions with Leu-263: the bifurcated H-bond between the threonine OH side chain and the N and CO (the latter through a water molecule) groups of Leu-263 (Fig. 9). Although the position of the OH (Thr-155) group is replaced by a water molecule in the mutated enzyme, the changes in the hydrogen bonding pattern produce two new interactions and, as a consequence, a less extended loop as observed by x-ray crystallography.

DISCUSSION

Effect of the Single Mutations at the 2′-Phosphate Interaction Site of $NADP^+$—The importance of a stabilizing interaction between the side chain of Ser-223 and the 2′-P of NADPH has been proven by replacement of this residue by a Gly, which lacks the OH group and, therefore, the hydrogen binding capability, and by an Asp, the residue that is highly conserved at the equivalent location in NADH-dependent enzymes (Table I; Fig. 1, *A* and *C*). Replacement of Ser-223 by either Gly or Asp produced enzymes that had only 0.5 and 0.005% of the catalytic efficiency of the WT FNR with NADPH (Table III, Fig. 3*A*), and the k_{obs} values for the reaction with NADPH were at least 30- and 1500-fold, respectively, slower than that of the WT enzyme when analyzed by stopped-flow (Fig. 5, Table V). However, no gross differences were detected for the catalytic parameters with NADH when compared with those of the WT enzyme (Fig. 3*B*). Thus, steady-state and fast kinetic studies suggest that removal of the Ser-223, and/or introduction of a negatively

TABLE V

Fast kinetic parameters for the reduction of the different Anabaena PCC 7119 FNR forms by NADPH and NADH as obtained by stopped-flow

All the reactions were carried out in 50 mM Tris/HCl, pH 8.0, at 25 °C and followed at 460 nm. The samples were mixed in the stopped-flow spectrometer at a final concentration of 6–11 μM for the FNR samples and 160–200 μM for NADPH or 2.5 mM for NADH.

FNR	NADPH		NADH	
	k_{obs1}	k_{obs2}	k_{obs1}	k_{obs2}
	s^{-1}	s^{-1}	s^{-1}	s^{-1}
WT	>500	200 ± 20	0.35 ± 0.05	0.005 ± 0.001
T155G	>400	80 ± 10	0.08 ± 0.01	0.012 ± 0.005
S223G	16 ± 1		ND[a]	
	2.0 ± 0.7[b]			
S223D	0.3 ± 0.1		0.21 ± 0.21	0.024 ± 0.005
	0.3 ± 0.1[b]			
R224Q	200 ± 20	20 ± 5	0.75 ± 0.05	
R233A	1.4 ± 0.6[b]		1.9 ± 0.5	
Y235F	300 ± 50	110 ± 20	0.57 ± 0.03	0.17 ± 0.02
Y235A	13 ± 1		0.05 ± 0.01	0.005 ± 0.001

[a] Not determined.

[b] Reactions studied with NADPH at 2.5 mM final concentration.

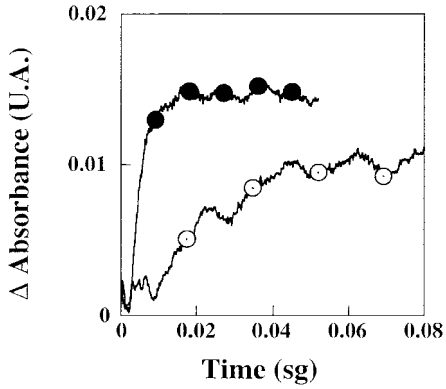

FIG. 6. **Time course of the anaerobic reactions of T155G FNR_{rd} with $NADP^+$.** Reaction of 7.5 μM T155G FNR_{rd} with 200 μM $NADP^+$ observed at 460 nm (*closed circles*) and 340 nm (*open circles*). Other conditions are as in Fig. 5. *U.A.*, units of absorbance.

charged residue at this position produces an enzyme that lacks its ability to discriminate between $NADP^+$/H and NAD^+/H. This behavior must be mainly due to the low affinity of both Ser-223 mutants for either $NADP^+$/H or NAD^+/H, as suggested from the fact that neither of them showed a difference spectrum in the presence of any of the oxidized coenzymes (Table IV). Thus, our studies confirm that Ser-223 side chain is a crucial determinant of FNR coenzyme specificity for NADPH. The very low degree of interaction between S223G and the coenzyme suggests that stabilization of NADPH binding must be due to a hydrogen bond or a charge-dipole interaction between the Ser-223-OH group and the 2′-P of $NADP^+$/H. Such interactions cannot be formed in this mutant. Moreover, introduction of a negative charge at position 223 almost completely prevents the FNR-$NADP^+$/H interaction. As mentioned above, the NAD^+/H-dependent enzymes of the FNR family have an aspartate residue at this position (Table I, Fig. 1). Several studies have already established the importance of such a negatively charged residue in NAD^+/H -dependent enzymes from different families as well as the strong alteration of the affinity for NAD^+/H when hydrogen bonds between this carboxylate group and the adenosine 2′- and 3′- hydroxyl positions of the coenzyme are not able to be formed (9, 40–42). It has also been shown that the introduction of such a negative charge at the residue that occupies the position spatially similar in some $NADP^+$/H-dependent enzymes prevents the interaction with the 2′-P of the coenzyme and might even enhance NAD^+/H affinity (43, 44). However, this latest effect has not been shown by our S223D mutant (Fig. 3*B*, Table V). Thus, it can be proposed that in the case of *Anabaena* FNR, the introduction of a negatively charged residue at position 223 produces a change in the catalytic behavior of the enzyme that is mainly due to the electrostatic repulsion between the negative side chain and the negatively charged 2′-P of $NADP^+$/H, which prevents its binding rather than allowing a favorable interaction of the Asp-233 with the 2′-OH group of NAD^+/H.

Previous studies suggest that the positively charged side chains of Arg-224 and Arg-233 might be involved in FNR coenzyme discrimination (15, 16, 24–26, 45–47). To test this hypothesis, the R224Q and R233A FNR mutants were produced by removing the positive charge. These enzymes were found to have 7.5 and 1.5%, respectively, the catalytic efficiency of the WT FNR with NADPH (Table III, Fig. 3*A*), and these low efficiencies are mainly due to the high K_m values for NADPH for these mutants. When analyzing the catalytic parameters with NADH for these mutants, both of them showed only a moderate increment in the k_{cat} value with regard to the WT FNR. Combination of these two factors produced a slight increment in their catalytic efficiencies with NADH (Table III, Fig. 3*B*). Both of these mutants elicited changes in their visible spectra upon $NADP^+$ addition (Fig. 4), indicating coenzyme binding. R224Q and R233A were estimated to bind $NADP^+$ 90- and 210-fold weaker than the WT FNR (Table IV). However, no affinity for NAD^+ was detected (Table IV). When analyzing the fast kinetic parameters of the reaction of NADPH with R224Q and R233A, different behaviors were detected for both mutants. R224Q shows a pattern of behavior similar to that of the WT enzyme but had k_{obs1} and k_{obs2} values at least 3 and 10 times smaller, respectively (Fig. 5, Table V). However, the reaction with R233A is more than 500-fold slower than that of the WT enzyme, even at high NADPH concentration. Finally, when these mutants were analyzed for the reaction with NADH, both reactions were best fit to monoexponential processes, with the observed rate constants for both of the mutants slightly higher than those observed for the WT enzyme (Table V). The obtained results indicate that replacement of Arg-224 by a Gln produces an enzyme that is still able to form a productive complex with NADPH, although considerably weaker, and to accept electrons efficiently from the coenzyme. This indicates that the function played by the guanidinium group of Arg-224 in stabilizing an interaction with the 2′-P could be also supported in a considerable degree by the Gln side chain. Moreover, a Gln residue at this position also slightly improves some of the processes studied with NADH. Analyzing sequence homology at this position allows the behavior observed for the R224Q mutant to be easily understood. As expected, all the $NADP^+$/H -dependent enzymes of the FNR family possess a positively charged residue at this position

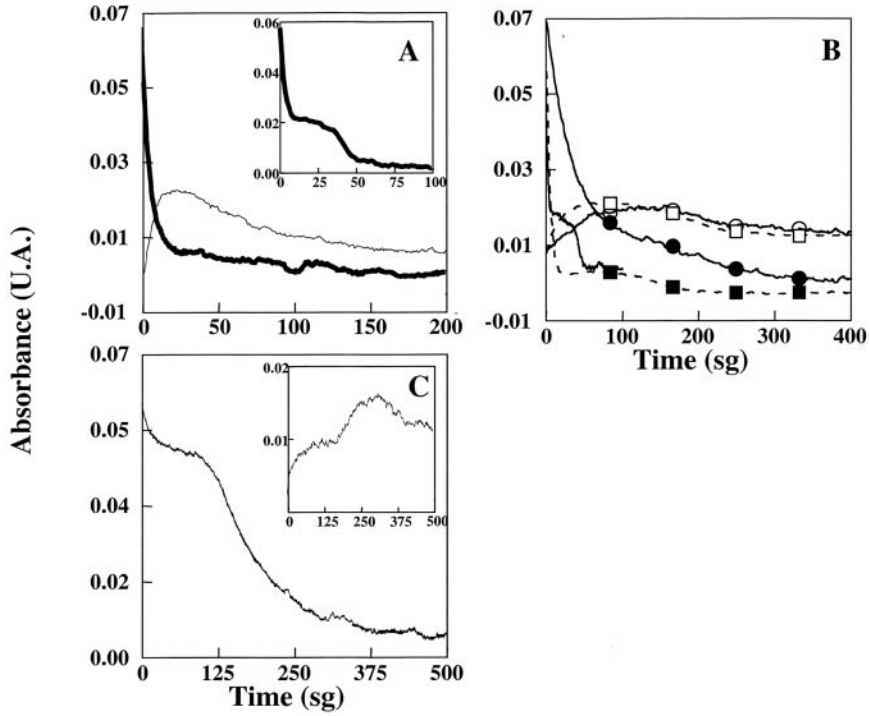

FIG. 7. **Time course of anaerobic reactions of the different FNR forms with NADH.** *A*, reaction of 9 μM WT FNR_{rd} with 2.4 mM NADH followed at 460 nm (*bold line*) and 600 nm (*thin line*). *B*, reaction of 9.5 μM S223D FNR_{rd} with 3.5 mM NADH observed at 460 nm (*closed squares*) and 600 nm (*open squares*), 10 μM Y235A FNR_{rd} with 2.8 mM NADH followed at 460 nm (*closed circles*), and 600 nm (*open circles*), and 8.5 μM Y235F with 2.4 mM NADH at 460 nm (*single thin line*). *C*, 10 μM T155G FNR_{rd} reacted with 2.7 mM NADH at 460 nm. The *inset* shows the same reaction observed at 600 nm. Other conditions are as in Fig. 5. *U.A.*, units of absorbance.

FIG. 8. **Stereo view of the Cα backbone superposition of FNR WT and T155G FNR mutant (*bold*).** Significant differences are concentrated not at the mutated position but in its environment (loop 261–268). The FAD cofactor and Thr-155 are represented as *sticks*. This figure was drawn using MOLSCRIPT (62).

TABLE VI
Selected non-conserved interactions between FNR WT and FNR T155G mutant

FNR WT		
Thr-155 Oγ	Leu-263 N	3.68 Å
Thr-155 Oγ	WAT601	2.94 Å
Thr-WAT601	Leu-263 O	3.11 Å
Gly-267 Oε2	Thr-302 Oγ	2.90 Å
FNR T155G mutant		
Leu-263 N	WAT552	3.66 Å
Leu-263 O	Met-266 N	3.60 Å
Glu-267 Oε2	Gly-265 N	3.03 Å

(Table I). Moreover, it is noteworthy that this is also the case for some of the NAD^+/H-dependent enzymes, and it is evident that in those enzymes that do not have negatively charged residues at this position, residues having side chains (Gln or His) capable of forming hydrogen bonds or dipole-charge interactions with the 2′-P are located at the equivalent position. Therefore, we can conclude that, although Arg-224 might be involved in an electrostatic interaction with the 2′-P that allows tighter binding to the substrate, it must be mainly involved in stabilization of the coenzyme binding through hydrogen bonds or charge-dipole interactions. However, this residue is not involved in determining FNR specificity for $NADP^+$/H *versus* NAD^+/H. Replacement of Arg-233 by an Ala produces a more drastic effect on the interaction between the enzyme with its natural coenzyme, $NADP^+$/H, which therefore affects the fast electron transfer process. This indicates that the side chain of the Ala is not able to provide some interactions that apparently allow an appropriate orientation of the coenzyme in its FNR binding region to allow subsequent electron transfer. Also, taking into account the conservation of a positively charged residue in all the $NADP^+$/H-dependent enzymes, and the fact that none of the NAD^+/H-dependent enzymes have a positively charged side chain at this position, our results suggest that the Arg-233 side chain provides stabilization of the 2′-P group and allows optimal $NADP^+$/H binding. However, removal of this interaction only slightly improves the affinity of the FNR for NAD^+/H. Positively charged residues equivalent to the aforementioned have already been shown to play a role in determining $NADP^+$/H specificity in other enzymes, such as cytochrome P-450 reductase or isocitrate dehydrogenase (48, 49).

The three-dimensional structural analysis of the complexes of FNR with $NADP^+$ also indicates a close interaction between the adenine moiety of the $NADP^+$ and the aromatic side chain of Tyr-235, which is conserved as a Tyr in all $NADP^+$/H-dependent enzymes and as a Phe in the NAD^+/H-dependent enzymes of the family (Fig. 1, Table I) (24, 26). The residue at this position of *Anabaena* FNR has been replaced either by a

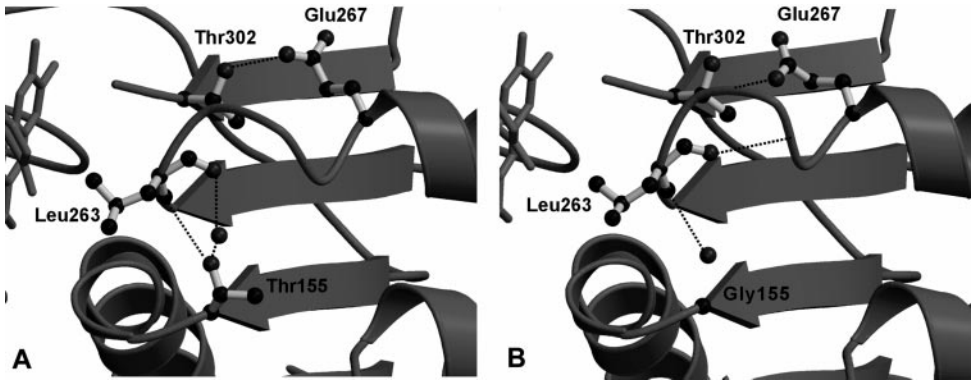

FIG. 9. **Hydrogen bond network and structural differences in the FNR WT (*A*) and in the T155G FNR mutant (*B*).** In the native state, OH (Thr-155) is making a bifurcated H-bond with the Leu-263 residue. Two new interactions are created after mutation: O (Leu-263) stabilizes a new interaction with N (Met-266), and Oϵ2 (Gly-267) stabilizes a new interaction with N (Gly-265). This produces a less extended conformation for the 261–268 loop in the mutated enzyme.

Phe or by an Ala. The diaphorase activities with NADPH for the Y235F and Y235A FNR enzymes were, respectively, 28% and just 0.3% of the WT catalytic efficiency (Table III, Fig. 3*A*). These results are mainly due to a 7-fold increment in the K_m of the Y235F form and to a 70-fold for the Y235A mutant, which was also accompanied by a 4-fold decrease of its k_{cat}. A slightly increment in the k_{cat} value of Y235F with NADH was also observed (Table III, Fig. 3*B*). On the contrary, Y235A was 4-fold less efficient with NADH than the WT. Moreover, whereas Y235F binds $NADP^+$ 35-fold weaker than the WT FNR (Fig. 4), no binding of this coenzyme was detected for Y235A. None of the mutants elicited a difference spectrum in the presence of NAD^+, indicating a very low affinity for this coenzyme (Table IV). Fast kinetic parameters of the reactions of either NADPH or NADH with Y235F and Y235A also show different behaviors for both mutants. Although Y235F behaved similarly to the WT enzyme, with only slightly slower observed rate constants (Figs. 5 and 7, Table V), the destabilizing effect introduced by the Ala at position 235 clearly resulted in a drastic decrease of the observed rate constant values of the processes. Therefore, our results clearly indicate that replacing Tyr-235 for a nonaromatic residue noticeably reduced the ability of FNR to interact efficiently with $NADP^+$/H, and it even produced a decrease in the already low affinity of the enzyme for NAD^+/H. This confirms that the stacking interaction between the aromatic residue at position 235 of *Anabaena* FNR and the adenine ring of $NAD(P)^+$/H is required to provide an adequate orientation between the protein and the coenzyme, which places the nicotinamide ring in a position capable of accepting electrons from the isoalloxazine ring. Our data also show that a Tyr at position 235 is much more efficient than a Phe for $NADP^+$/H binding and electron transfer, confirming the importance of the hydrogen bond between the Tyr-OH and the 2′-P of $NADP^+$/H in complex formation and orientation. The lack of this hydrogen bond in the Y235F mutant still allows $NADP^+$/H binding but results in a weaker and less productive complex. On the other hand it is noticeable that this latter mutant appears to accommodate NAD^+/H more efficiently. This might also be expected, taking into account that the NADH-dependent members of the enzyme have a Phe at this position (Table I, Fig. 1*D*).

Effect of the Single Mutation T155G—Thr-155 of *Anabaena* FNR was replaced by a Gly, the residue present at the equivalent position in all NAD^+/H -dependent members of the family (Fig. 1, Table I), to test if this residue and the region that contains it is involved in coenzyme specificity and if NAD^+/H binding could be induced. This mutation produced only a slight effect on the catalytic properties of the enzyme when its reactivity was assayed with NADPH either by steady-state or by fast kinetic methods (Table III and V, Fig. 3). The K_m for NADPH and K_d for the T155G-$NADP^+$ complex suggest that these changes must be due to a decrease in the affinity for the coenzyme (Tables III and IV). The latest analysis also indicates that this mutant accommodates the $NADP^+$/H coenzyme in a different orientation with regard to the flavin ring than the WT (Fig. 4). Analysis of the T155G FNR three-dimensional structure indicates that the introduced mutation produces an alteration of a hydrogen bond network (Fig. 9), which produces a slight displacement of the backbone in the $NADP^+$ binding domain (Fig. 8). In particular, important structural differences are observed in the loop comprising residues 261–268. Interestingly, the three-dimensional structural analysis of this region in the different members of the FNR family shows that in the case of NAD^+/H-dependent enzymes a different organization of the hydrogen bond network (Fig. 9) and a hairpin-like region rich in proline residues (Table I, Fig. 10) are present. This analysis also shows that the conformation of such a region rich in proline residues in the NAD^+/H members would not be compatible with the presence of a Thr (or Pro) at the position equivalent to 155 of *Anabaena* FNR in the $NADP^+$/H-members due to steric hindrance (Fig. 10). Replacement of Thr-155 in *Anabaena* FNR by a Gly produces a slight retraction of the loop that might explain some of the behaviors observed for this mutant such as the increase in its affinity for NAD^+/H, as

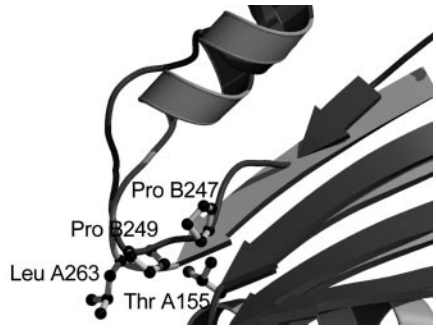

FIG. 10. **MOLSCRIPT drawing of the superposition of *Anabaena* FNR (*light*) and NADH-cytochrome b_5 reductase (*dark*) (58) near the position of residue 155.** In the NAD^+/H-dependent enzymes, a Gly residue at this position is favored due to the presence of a hairpin-like region (formed by a series of prolines) that will not allow the space for a Thr to occupy position 155 of FNR. On the contrary, the absence of this hairpin in the $NADP^+$/H-dependent enzymes permits the presence of residues such as Thr or Pro at this position. Relevant residues are labeled as chain A in FNR or chain B in cytochrome b_5 reductase.

indicated by the decrease observed in the K_m for NADH and by the fact that of all the FNR forms assayed, T155G was the only one that showed a difference spectra upon NAD^+ binding (Fig. 4*C*). However, the mutant did not enhance reactivity with NADH, as shown by the very small values obtained by k_{cat} and k_{obs} when studied by steady-state and by fast kinetic methods (Table III and V). This indicates that, although the structural modifications induced by a Gly at position 155 enhance the enzyme affinity for NAD^+/H, the resulting complex does not provide an orientation conducive to electron transfer. This was expected, since the other regions of the protein that determine the coenzyme specificity are involved in $NADP^+$/H recognition.

General Conclusions—The analysis of the determinants of coenzyme specificity in *Anabaena* FNR indicates that all the residues interacting with the 2′-P group of NADPH, Ser-223, R224, Arg-233, and Y235, are not involved to the same extent in determining coenzyme affinity and specificity. Thus, the side chain of Ser-223 is crucial in determining $NADP^+$/H binding, with the presence of a negatively charged residue at this position preventing its binding. Although the presence of a positively charged residue at positions 224 and 233 of *Anabaena* FNR are not crucial in determining coenzyme specificity, these residues are involved in providing a stronger interaction between the enzyme and $NADP^+$/H. The importance of an aromatic residue at position 235 of *Anabaena* FNR for the interaction with both coenzymes, $NADP^+$/H and NAD^+/H, has been demonstrated, as has the fact that a hydrogen bond between the coenzyme and the OH group of Tyr-235 is also involved in determining the $NADP^+$/H *versus* NAD^+/H specificity in FNR. Finally, our results also indicate that the determinants of coenzyme specificity of FNR are not only situated in the 2′-P binding region, but that other regions of the protein must be involved. Thus, the arrangement of the backbone chain in the coenzyme binding domain around the loop that connects strand 4 and the α-helix D in *Anabaena* FNR must be one of the regions which determines coenzyme specificity.

Acknowledgments—We are grateful to Prof. R. Perham, University of Cambridge and also to Dr. J. K. Hurley and Prof. G. Tollin, University of Arizona, for their collaboration in many aspects of this work.

REFERENCES

1. Clarke, A. R., Atkinson, T., and Holbrook, J. J. (1989) *Trends Biochem. Sci.* **14,** 101–105, 145–148
2. Hedstrom, L. (1994) *Curr. Opin. Struct. Biol.* **4,** 608–611
3. Scrutton, N. S., Berry, A., and Perham, R. N. (1990) *Nature* **343,** 38–43
4. Friesen, J. A., Lawrence, C. M., Stauffacher, C. V., and Rodwell, V. W. (1996) *Biochemistry* **35,** 11945–11950
5. Chen, R., Greer, A., and Dean, A. M. (1996) *Proc. Natl. Acad. Sci. U. S. A.* **93,** 12171–12176
6. Zubay, G. L. (1998) *Biochemistry*, 4th Ed., Wm. C. Brown Publishers, Dubuque, IA
7. Rossmann, M., Moras, D., and Olsen, K. (1974) *Nature* **250,** 194–199
8. Karplus, P. A., Daniels, M. J., and Herriott, J. R. (1991) *Science* **251,** 60–66
9. Didierjean, C., Rahuel-Clermont, S., Vitoux, B., Dideberg, O., Branlant, G., and Aubry, A. (1997) *J. Mol. Biol.* **268,** 739–759
10. Arakaki, A. K., Ceccarelli, E. A., and Carrillo, N. (1997) *FASEB. J.* **11,** 133–140
11. Batie, C. J., and Kamin, H. (1986) *J. Biol. Chem.* **261,** 11214–11223
12. Sancho, J., and Gómez-Moreno, C. (1991) *Arch. Biochem. Biophys.* **288,** 231–238
13. Piubelli, L., Aliverti, A., Arakaki, A. K., Carrillo, N., Ceccarelli, E. A., Karplus, P. A., and Zanetti, G. (2000) *J. Biol. Chem.* **275,** 10472–10476
14. Walker, M. C., Pueyo, J. J., Navarro, J. A., Gómez-Moreno, C., and Tollin, G. (1991) *Arch. Biochem. Biophys.* **287,** 351–358
15. Medina, M., Méndez, E., and Gómez-Moreno, C. (1992) *FEBS Lett.* **298,** 25–28
16. Medina, M., Méndez, E., and Gómez-Moreno, C. (1992b) *Arch. Biochem. Biophys.* **299,** 281–286
17. Medina, M., Martínez-Júlvez, M., Hurley, J. K., Tollin, G., and Gómez-Moreno, C. (1998) *Biochemistry* **37,** 2715–2728
18. Martínez-Júlvez, M., Hermoso, J., Hurley, J. K., Mayoral, T., Sanz-Aparicio, J., Tollin, G., Gómez-Moreno, C., and Medina, M. (1998) *Biochemistry* **37,** 17680–17691
19. Hurley, J. K., Fillat, M. F., Gómez-Moreno, C., and Tollin, G. (1996) *J. Am. Chem. Soc.* **118,** 5526–5531
20. Hurley, J. K., Weber-Main, A. M., Stankovich, M. T., Benning, M. M., Thoden, J. B., Vanhooke, J. L., Holden, H. M., Chae, Y. K., Xia, B., Cheng, H., Markley, J. L., Martínez-Júlvez, M., Gómez-Moreno, C., Schmeits, J. L., and Tollin, G. (1997) *Biochemistry* **36,** 11100–11117
21. Orellano, E. G., Calcaterra, N. B., Carrillo, N., and Ceccarelli, E. A (1993) *J. Biol. Chem.* **268,** 19267–19273
22. Aliverti, A., Bruns, C. M., Pandini, V. E., Karplus, P. A., Vanoni, M. A., Curti, B., and Zanetti, G. (1995) *Biochemistry* **34,** 8371–8379
23. Aliverti, A., Deng, Z., Ravasi, D., Piubelli, L., Karplus, P. A., and Zanetti, G. (1998) *J. Biol. Chem.* **273,** 34008–34015
24. Serre, L., Vellieux, F. M. D., Medina, M., Gómez-Moreno, C., Fontecilla-Camps, J. C., and Frey, M. (1996) *J. Mol. Biol.* **263,** 20–39
25. Bruns, C. M., and Karplus, P. A. (1995) *J. Mol. Biol.* **247,** 125–145
26. Deng, Z., Aliverti, A., Zanetti, G., Arakaki, A. K., Ottado, J., Orellano, E. G., Calcaterra, N. B., Ceccarelli, E. A., Carrillo, N., and Karplus, A. (1999) *Nat. Struct. Biol.* **6,** 847–853
27. Correll, C. C., Ludwig, M. L., Bruns, C. M., and Karplus, P. A. (1993) *Protein Sci.* **2,** 2112–2133
28. Madoz-Gúrpide, J., Abad, J. M., Fernández-Recio, J., Vélez, M., Vázquez, L., Gómez-Moreno, C., and Fernández, V. M. (2000) *J. Am. Chem. Soc.* **122,** 9808–9817
29. Morales, R., Charon, M.-H., Kachalova, G., Serre, L., Medina, M., Gómez-Moreno, C., and Frey, M. (2000) *EMBO Rep.* **1,** 271–276
30. Gómez-Moreno, C., Martínez-Júlvez, M., Fillat, M. F., Hurley, J. K., and Tollin, G. (1995) in *Photosynthesis: from Light to Biosphere* (Mathis, P., ed) Vol. II, pp. 627–632, Kluwer Academic Publishers Group, Dordrecht, Netherlands
31. Leslie, A. G. W. (1987) *Proceedings of the CCP4 Study Weekend* (Helliwell, J. R., Machin, P. A., and Papiz, M. Z., eds) pp. 39–50, SERC Daresbury Laboratory, Warrington, United Kingdom
32. Collaborative Computational Project, Number 4. (1994) *Acta Crystallogr. Sect. D Biol. Crystallogr.* **50,** 760–763
33. Navaza, J. (1994) *Acta Crystallogr. Sect. A* **50,** 157–163
34. Castellano, E., Oliva, G., and Navaza, J. (1992) *J. Appl. Crystallogr.* **25,** 281–284
35. Brünger, A. T. (1993) *X-PLOR: A System for X-ray Crystallography and NMR*, Yale University Press, New Haven, CT
36. Jones, T. A., Zou, J. Y., Cowan, S. W., and Kjeldgaard, M. (1991) *Acta Crystallogr. Sect. A* **47,** 110–119
37. Brünger, A. T. (1992) *Nature* **355,** 472–474
38. Pueyo, J. J., and Gómez-Moreno, C. (1991) *Prep. Biochem.* **21,** 191–204
39. Batie, C. J., and Kamin, H. (1984) *J. Biol. Chem.* **259,** 11976–11985
40. Holmberg, N., Ryde, U., and Bülow, L. (1999) *Protein Eng.* **12,** 851–856
41. Chen, Z., Lee, W. L., and Chang, S. H. (1991) *Eur. J. Biochem.* **202,** 263–267
42. Fan, F., Lorenzen, J. A., and Plapp, B. V. (1991)*Biochemistry* **30,** 6397–6401
43. Nakanishi, M., Matsuura, K., Kaibe, H., Tanaka, N., Nonaka, T., Mitsui, Y., and Hara, A. (1997) *J. Biol. Chem.* **272,** 2218–2222
44. Hurley, J. H., Chen, R., and Dean, A. M. (1996) *Biochemistry* **35,** 5670–5678
45. Aliverti, A., Lúbberstedt, T., Zanetti, G., Herrmann, R. G., and Curti, B. (1991) *J. Biol. Chem.* **266,** 17760–17763
46. Zanetti, G., Gozzer, C., Sachi, G., and Curti, B. (1979) *Biochim. Biophys. Acta* **569,** 127–134
47. Zanetti, G. (1976) *Biochim. Biophys. Acta* **445,** 14–24
48. Sem, D. S., and Kasper, C. B. (1993) *Biochemistry* **32,** 11548–11558
49. Yaoi, T., Miyazaki, K., and Oshima, T. (1994) *FEBS Lett.* **355,** 171–172
50. Fillat, M. F., Bakker, H. A. C., and Weisbeek, P. J. (1990) *Nucleic Acids Res.* **18,** 7161
51. Newman, B. J., and Gray, J. C. (1988) *Plant Mol. Biol.* **10,** 511–520
52. Karplus, P. A., Walsh, K. A., and Herriott, J. R. (1984) *Biochemistry* **23,** 6576–6583
53. Porter, T. D., and Kasper, C. B. (1985) *Proc. Natl. Acad. Sci. U. S. A.* **82,** 973–977
54. Ostrowski, J., Barber, M. J., Rueger, D. C., Miller, B. E., Siegel, L. M., and Kredich, N. M. (1989) *J. Biol. Chem.* **264,** 15796–15808
55. Hall, A. V., Antoniou, H., Wang, Y., Cheung, A. H., Arbus, A. M, Olson, S. L., Lu, W. C., Kau, C. L., and Marsden, P. A. (1994) *J. Biol. Chem.* **269,** 33082–33090
56. Long, D. M., Oaks, A., and Rothstein, S. J. (1992) *Physiol. Plant.* **85,** 561–566
57. Hyde, G. E., and Campbell, W. H. (1990) *Biochem. Biophys. Res. Commun.* **168,** 1285–1291
58. Ozols, J., Korza, G., Heinemann, F. S., Hediger, M. A., and Strittmatter, P. (1985) *J. Biol. Chem.* **260,** 11953–11961
59. Nishida, H., Inaka, K., Yamanaka, M., Kaida, S., Kobayashi, K., and Miki, K. (1995) *Biochemistry* **34,** 2763–2767
60. Correll, C. C., Batie, C. J., Ballou, D. P., and Ludwig, M. L. (1992) *Science* **258,** 1604–1610
61. Kraulis, P. J. (1991) *J. Appl. Crystallogr.* **24,** 946–950
62. Merrit, E. A., and Murphy, M. E. P. (1994) *Acta Crystallogr. Sect. D Biol. Crystallogr.* **50,** 869–873